Evaluating China's fossil-fuel CO2 emissions from a comprehensive dataset of nine inventories

Pengfei Han[1*], Ning Zeng[2*], Tom Oda[3], Xiaohui Lin[4], Monica Crippa[5], Dabo Guan[6,7], Greet Janssens-Maenhout[5], Xiaolin Ma[8], Zhu Liu[6,9], Yuli Shan[10], Shu Tao[11], Haikun Wang[8], Rong Wang[11,12], Lin Wu[4] , Xiao Yun[11], Qiang Zhang[13], Fang Zhao[14], Bo Zheng[15]

[1]State Key Laboratory of Numerical Modeling for Atmospheric Sciences and Geophysical Fluid Dynamics, Institute of Atmospheric Physics, Chinese Academy of Sciences, Beijing, China

[2]Department of Atmospheric and Oceanic Science, and Earth System Science Interdisciplinary Center, University of Maryland, College Park, Maryland, USA

[3]Goddard Earth Sciences Research and Technology, Universities Space Research Association, Columbia, MD, United States

[4]State Key Laboratory of Atmospheric Boundary Layer Physics and Atmospheric Chemistry, Institute of Atmospheric Physics, Chinese Academy of Sciences, Beijing, China

[5]European Commission, Joint Research Centre (JRC), Directorate for Energy, Transport and Climate, Air and Climate Unit, Ispra (VA), Italy

[6]Department of Earth System Science, Tsinghua University, Beijing, China

[7]Water Security Research Centre, School of International Development, University of East Anglia, Norwich, UK

[8]State Key Laboratory of Pollution Control and Resource Reuse, School of the Environment, Nanjing University, Nanjing, China

[9]Tyndall Centre for Climate Change Research, School of International Development, University of East Anglia, Norwich, UK

[10]Energy and Sustainability Research Institute Groningen, University of Groningen, Groningen 9747 AG, Netherlands

[11]Laboratory for Earth Surface Processes, College of Urban and Environmental Sciences, Peking University, Beijing, China

[12]Department of Environmental Science and Engineering, Fudan University, Shanghai, China

[13]Ministry of Education Key Laboratory for Earth System Modeling, Department of Earth System Science, Tsinghua University, Beijing, China

[14]Key Laboratory of Geographic Information Science (Ministry of Education), School of Geographic Sciences, East China Normal University, Shanghai, China

[15]Laboratoire des Sciences du Climat et de l'Environnement, CEA-CNRS-UVSQ, UMR8212, Gif-sur-Yvette, France

Correspondence to: Pengfei Han (pfhan@mail.iap.ac.cn); Ning Zeng (zeng@umd.edu)

Abstract. China's fossil-fuel CO_2 emissions ($FFCO_2$) account for about 28% of the global total $FFCO_2$ in 2016. An accurate estimate of China's $FFCO_2$ is a prerequisite for global and regional carbon budget analyses and monitoring of carbon emission reduction efforts. However, large uncertainties and discrepancies exist in China's $FFCO_2$ estimations due to lack of detailed traceable emission factors and multiple statistical data sources. Here, we evaluated China's $FFCO_2$ emissions from 9 published global and regional emission datasets. These datasets show that the total emission increased from 3.4 (3.0-3.7) in 2000 to 9.8 (9.2-10.4) Gt CO_2 yr^{-1} in 2016. The variations in their estimates were due largely to the different emission factors (EF) (0.491-0.746 t C per t of coal) and activity data. The large-scale patterns of gridded emissions showed a reasonable agreement with high emissions concentrated in major city clusters, and the standard deviation mostly ranged 10-40% at provincial level.

However, patterns beyond the provincial scale vary greatly with the top 5% of grid-level account for 50-90% of total emissions for these datasets. Our findings highlight the significance of using locally-measured EF for the Chinese coals. To reduce the uncertainty, we call on the enhancement of physical CO_2 measurements and use them for datasets validation, key input data sharing (e.g. point sources) and finer resolution validations at various levels.

Keywords: fossil-fuel CO_2 emissions, spatial disaggregation, emission factor, activity data, comprehensive dataset

1 Introduction

Anthropogenic emission of carbon dioxide (CO_2) is one of the major contributions in accelerating global warming (IPCC, 2007). The global CO_2 emissions from fossil fuel combustion and industry processes increased to 36.23 Gt CO_2 yr^{-1} in 2016, with a mean growth rate of 0.62 Gt CO_2 yr^{-1} per year over the last decade (Le Quéré et al., 2018). In 2006, China became the world largest emitter of CO_2 (Jones, 2007). The CO_2 emission from fossil fuel combustion and cement production of China was 9.9 Gt CO_2 in 2016, accounting for about 28% of all global fossil-fuel based CO_2 emissions (Le Quéré et al., 2018;IPCC AR5, 2013). To avoid the potential adverse effects from climate change (Zeng et al., 2008;Qin et al., 2016), the Chinese government has pledged to peak its CO_2 emissions by 2030 or earlier and to reduce the CO_2 emission per unit gross domestic product (GDP) by 60-65% below 2005 levels (SCIO, 2015). Thus, an accurate quantification of China's CO_2 emissions is the first step in understanding its carbon budget and making carbon control policy.

Chinese total emission estimates are thought to be uncertain or biased due to the lack of reliable statistical data and/or the use of generic emission factors (EF) (e.g. (Guan et al., 2012); (Liu et al., 2015b)). National and provincial data based inventories used activity data from different sources. The Carbon Dioxide Information Analysis Center (CDIAC) used national energy statistics from United Nations (UN) (Andres et al., 2012), and both the Open-Data Inventory for Anthropogenic Carbon dioxide (ODIAC) and Global Carbon Project (GCP) mainly use CDIAC total estimates and thus they are identical in time series (Le Quéré et al., 2018;Oda et al., 2018). The Emissions Database for Global Atmospheric Research (EDGAR) and Peking University CO_2 (PKU-CO_2, hereafter named as PKU) derived emissions from the energy balance statistics of the International Energy Agency (IEA) (Janssens-Maenhout et al., 2019a;Wang et al., 2013). On the other hand, provincial data based inventories developed within China all used provincial energy balance sheet in China Energy Statistics Yearbook (CESY) from National Bureau of Statistics of China (NBS) (Cai et al., 2018;Liu et al., 2015a;Liu et al., 2013;Shan et al., 2018). As for EF, there are generally four sources, i.e., 1) The Intergovernmental Panel on Climate Change (IPCC) default values that has been adopted by ODIAC and EDGAR (Andres et al., 2012;Janssens-Maenhout et al., 2019b;Oda et al., 2018); 2) National Development and Reform Commission (NDRC) (NDRC, 2012b); 3) China's National Communication, which reported to the United Nations Framework Convention on Climate Change (UNFCCC) (NDRC, 2012a); 4) The China Emission Accounts and Datasets (CEADs) EF that are locally optimized through large sample measurements (Liu et al., 2015b). The existing estimates of global total $FFCO_2$ emissions are comparable in magnitude, with an uncertainty generally

within ±10% (Le Quéré et al., 2018;Oda et al., 2018). However, there are great differences at national scale (Marland et al., 2010;Olivier et al., 2014), with the uncertainty ranging from a few percent to more than 50% in estimated emissions for individual countries (Andres et al., 2012;Boden et al., 2016;Oda et al., 2018).

Along with the total emissions estimates, spatial distributions are also important for several reasons: 1) Spatial gridded products provide basic understandings on CO_2 emissions; 2) They are key inputs (as priors) for transport and data assimilation models and influenced the carbon budget (Bao et al., 2020); 3) For high emissions areas recognized by multiple inventories, they can be used for policy making in emissions reductions and can provide useful information for deployment of instruments in emissions monitoring (Han et al., 2020). At the global level, gridded emission datasets are often based on disaggregation of country scale emissions (Janssens-Maenhout et al., 2017;Wang et al., 2013). Thus, the gridded emissions are subjected to errors and uncertainties from the total emission calculation and emission spatial disaggregation (Andres et al., 2016;Oda et al., 2018;Oda and Maksyutov, 2011). For example, the Carbon Dioxide Information Analysis Center (CDIAC) distributes national energy statistics at a resolution of 1 °×1 ° using population density as a proxy (Andres et al., 2016;Andres et al., 2011). Further, to improve spatial resolution of emission inventory, the Open-Data Inventory for Anthropogenic Carbon dioxide (ODIAC) distributes national emissions based on CDIAC and BP statistics with satellite nighttime lights and power plant emissions (Oda et al., 2018;Oda and Maksyutov, 2011). (EDGAR) derived emissions from the energy balance statistics of the International Energy Agency (IEA), and country specific activity datasets from BP plc, United States Geological Survey (USGS), World Steel Association, Global Gas Flaring Reduction Partnership (GGFR)/U.S. National Oceanic and Atmospheric Administration (NOAA) and International Fertilizer Association (IFA). Gridded emission maps at 0.1 °x0.1 °were produced using spatial proxy data based on the population density, traffic networks, nighttime lights and point sources as described in Janssens-Maenhout et al. (2017). Based on the sub-national fuel data, population and other geographically resolved data, a high-resolution inventory of global CO_2 emissions was developed at Peking University (Wang et al., 2013). .

In order to accurately calculate emissions, a series of efforts have been conducted to quantitatively evaluate China's CO_2 emissions using national or provincial activity data, local EF, and detailed data set of point sources (Cai et al., 2018;Li et al., 2017;Wang et al., 2013). The China High Resolution Emission Database (CHRED) was developed by Cai et al. (2018) and Wang et al. (2014) based on the provincial statistics, traffic network, point sources and industrial and fuel-specific EF. CHRED was featured by its exclusive point source data for 1.58 million industrial enterprises from the First China Pollution Source Census. The Mutli-resolution Emission Inventory for China (MEIC) was developed by Qiang et al. (2007), Lei et al. (2011) and Liu et al. (2015a) at Tsinghua University through integrating provincial statistics, unit-based power plant emissions, population density, traffic networks, and emission factor (EF) (Li et al., 2017;Zheng et al., 2018b;Zheng et al., 2018a). MEIC used China Power Emissions Database (CPED), and the unit-based approach is used to calculate emissions

for each coal-fired power plant in China with detailed unit-level information (e.g., coal use, geographical coordinates). For the mobile sources, a high-resolution mapping approach is adopted to constrain the vehicle emissions using county-level activity database. CEADs was constructed by (Shan et al., 2018;Shan et al., 2016) and Guan et al. (2018) based on different levels of inventories to provide emissions at national and provincial scales. CEADs used coal EF from the large-sample measurements (602 coal samples and samples from 4,243 coal mines). And this is assumed to be more accurate than the IPCC default EFs.

Regardless of these efforts, however, the amount of China's CO_2 emissions remains uncertain due to the large discrepancy among current estimates, of which the difference ranges from 8-24% of the total estimates (Shan et al., 2018;Shan et al., 2016). Several studies made efforts of quantifying the possible uncertainty in China's $FFCO_2$, such as differences from estimation approaches (Berezin et al., 2013), energy statistics (Hong et al., 2017;Han et al., 2020), spatial scales (Wang and Cai, 2017), and point source data . Importantly, the authors would like to point out that the lack of a comprehensive understanding and comparison of the potential uncertainty in estimates of China's $FFCO_2$, including spatial, temporal, proxy, and magnitude components, makes Chinese emissions possible more uncertain, and thus it is important to present, analyze and explain such differences among inventories .

Here we evaluated the uncertainty in China's $FFCO_2$ estimates by synthesizing global gridded emissions datasets (ODIAC, EDGAR, and PKU) and China-specific emission maps (CHRED, MEIC, and the Nanjing University CO_2 (NJU) emission inventory). Moreover, several other inventories were used in the evaluation analysis, such as the Global Carbon Budget from the Global Carbon Project, the National Communication on Climate Change of China (NCCC).

The purposes of this study were to: 1) quantify the magnitude and the uncertainty in China's $FFCO_2$ estimates using the spread of values from the state-of-the-art inventories; 2) identify the spatiotemporal differences of China's $FFCO_2$ emissions between the existing emission inventories and explore the underlying reasons for such differences. To our knowledge, this is the first comprehensive evaluation of the most up-to-date and mostly publicly available carbon emission inventories for China.

2. Emissions data

The evaluation analysis was conducted from 6 gridded datasets (listed in Table 1) and 3 other statistical data. We selected year 2012 for spatial analysis since this is the most recent year available for all gridded data sets and also this is a peak year of emissions due to the strong reductions from impacts of the 12th-Five-Year-Plan. Specifically, the global fossil fuel CO_2 emission datasets included the year 2017 version of ODIAC (ODIAC2017), the version v4.3.2 of EDGAR (EDGARv4.3.2), PKU-CO_2, which all used the Carbon Monitoring for Action (CARMA) as point source. The China-specific emission data used were the year 2007 of CHRED, the MEIC v1.3, NJU-CO_2 v2017, which all used China Energy Statistical Yearbook

(CESY) activity data. Moreover, 3 inventories were used as a reference, i.e., GCP/CDIAC, CEADs and NCCC, since GCP and ODIAC used CDIAC for most of the years, except for the recent two years that were extrapolated by BP data, these three were treated as one in time series comparison. Data were collected from official websites for ODIAC, EDGAR, PKU and 6 tabular statistic data, and were acquired from their authors for CHRED, MEIC and NJU. See supporting information for more details on data sources and methodology of each dataset.

3. Methodology for evaluation of multiple datasets

We evaluated these datasets from three aspects: data sources, boundary (emission sectors) and methodology (Figure 1, Table 1 and S1, S2). For data source, there are two levels: national data such as UN or IEA statistics and provincial level data such as CESY. The emission sectors mainly include fossil fuel production, industry production and processes, households, transportation, aviation/shipping, agriculture, natural biomass burning from wild fire and waste for these datasets, and Table S1 listed sectors included in each inventory. And for methodology, analysis of inventories includes total estimates (activity data and EF) aspect and spatial disaggregation of point, line and area sources. As Fig. 1 depicted the conceptual procedure in total emissions estimates and how gridded maps are produced for all inventories, it is important to know the differences in activity data, EF and spatial proxy data and spatial disaggregation methods they used, to understand the differences among inventories in total emissions estimates and spatial characteristics.

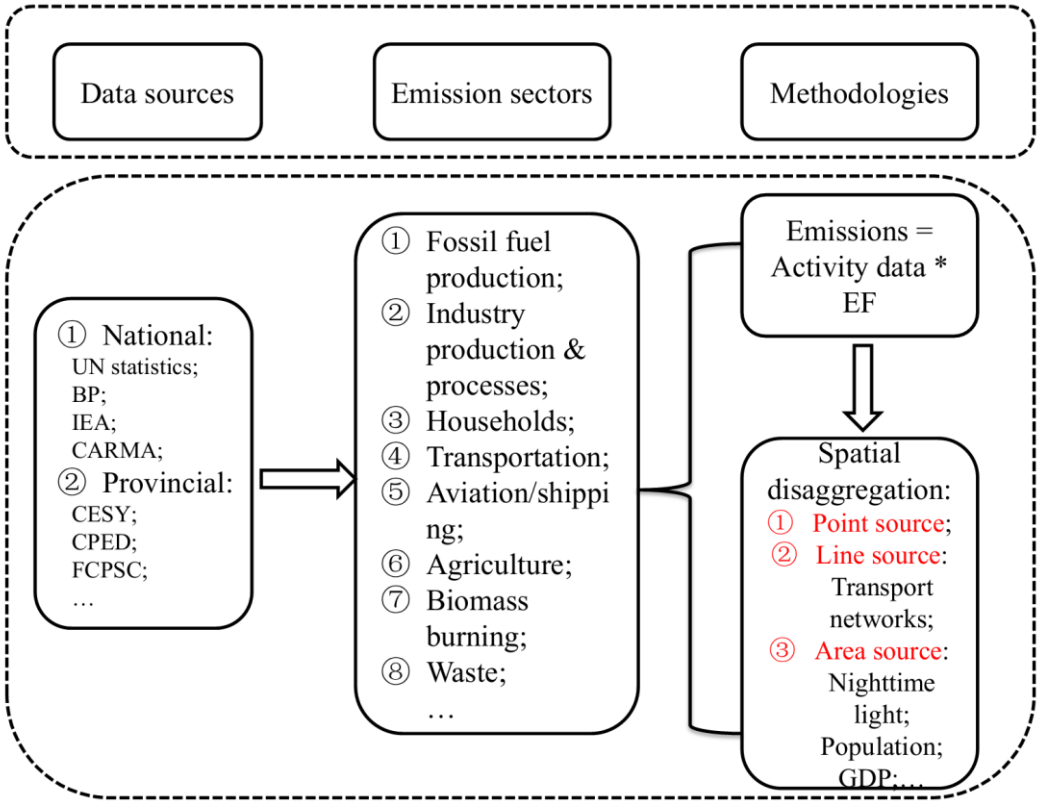

Figure 1 Conceptual diagram for data evaluation based on data sources, emission sectors and methodologies.

Preprocessing of six gridded CO_2 emission datasets included several steps that are described as follows. First, The global map of CO_2 emissions (i.e. ODIAC, EDGAR and PKU) were re-projected to Albers Conical Equal Area projection (that of CHRED). And the nearest neighbor algorithm was used to resample different spatial resolution into a pixel size of 10 km by 10 km, and this method takes the value from the cell closest to the transformed cell as the new value. Second, the national total emissions were derived using ArcGIS zonal statistics tool for CHRED while the others were from tabular data provided by data owners. Finally, the grids for each inventory were sorted in ascending order and then plotted on a logarithmic scale to represent the distribution of emissions. To identify the contribution of high emission grids, emissions at grid level that exceeded 50 kt CO_2 yr^{-1} km^{-2} and the top 5% emitting grids were selected for analysis.

156 Table 1 General information for emission data sets*

Data	ODIAC2017	EDGARv432	PKU	CHRED	MEIC	NJU	CEADs	GCP/CDIAC	NCCC
Domain	Global	Global	Global	China	China	China	China	Global	China
Temporal coverage	2000-2016	1970-2012	1960-2014	2007, 2012	2000-2016	2000-2015	1997-2015	1959-2018	2005, 2012, 2014
Temporal resolution	Monthly	Annual	Monthly	Biennially or triennially	Monthly	Annual	Annual	Annual	Annual
Spatial resolution	1 km	0.1 degree	0.1 degree	10 km	0.25 degree	0.25 degree	N/A	N/A	N/A
Emission estimates	Global & National	Global & National	Global & National	National & Provincial	National & Provincial	National & Provincial	National & Provincial	Global & National	National
Emission factor for raw coal (tC per t of coal)	0.746	0.713	0.518	0.518	0.491	0.518	0.499	0.746	0.491
Uncertainty	17.5% (95% CI)	±15%	±19% (95% CI)	±8%	±15%	7-10% (90% CI)	-15% - 25% (95% CI)	17.5% (95% CI)	5.40%
Point	CARMA	CARMA3.0	CARMA2.0	FCPSC	CPED	CEC;A	N/A	N/A	N/A

source	2.0					CC;CCTEN			
Line source	N/A	the OpenStreetMap and OpenRailwayMap, Int. aviation and bunker	N/A	The national road, railway, navigation network, and traffic flows	Transport networks	N/A	N/A	N/A	N/A
Area source	Nighttime light	Population density, nighttime light	Vegetation and population density, nighttime light	Population density, land use, human activity	Population density, land use	Population density, GDP	N/A	N/A	N/A
Version name	ODIAC2017	EDGARv4.3.2_FT2016，EDGARv4.3.2	PKU-CO2-v2	CHRED	MEIC v.1.3	NJU-CO$_2$v2017	CEADs	N/A	N/A
Year published/ updated	2018	2017	2016	2017	2018	2017	2017	2019	2018

Data sources	http://db.cger.nies.go.jp/dataset/ODIAC/	http://edgar.jrc.ec.europa.eu/overview.php?v=432_GHG&SECURE=123	http://inventory.pku.edu.cn/download/download.html	Data developer	Data developer	Data developer	http://www.ceads.net/ (registration requred)	https://www.globalcarbonproject.org/carbonbudget/19/data.htm	https://unfccc.int/sites/default/files/resource/China 2BUR_English.pdf
References	Oda (2018)	Janssens-Maenhout (2017)	Wang et al., 2013	Cai et al. (2018); Wang et al. (2014)	Zheng (2018); Liu et al. (2015)	Liu (2013)	Shan et al. (2018)	Friedlingstein et al. (2019)	NCCC (2018)

157 * CI: Confidence interval; FCPSC: the First China Pollution Source Census; CPED: China Power Emissions Database; CEC: Commission for Environmental Cooperation;

158 ACC: China Cement Almanac; CCTEN: China Cement Industry Enterprise Indirectory; GDP: Gross domestic product; N/A: Not available.

4. Results

4.1 Total emissions and recent trends

The interannual variations of China's CO_2 emissions from 2000 to 2016 were evaluated from 6 gridded emission maps and 3 national total inventories (Figure 2). All datasets show a significant increasing trend in the period of 2000 to 2013 from 3.4 to 9.9 Gt CO_2. The range of the 9 estimates increased simultaneously from 0.7 to 2.1 Gt CO_2 (both are 21% of the corresponding years' total emissions). In the second period (from 2013 to 2016), the temporal variations mostly levelled off or even decreased. Specifically, the emissions estimated from PKU and CEADs showed a slight downward trend although they used independent activity data of IEA (2014) and Statistics (2016), and this downward trend is attributed to changes in industrial structure, improved combustion efficiency, emissions control and slowing economic growth (Guan et al., 2018;Zheng et al., 2018a).

There is a large discrepancy among the current estimates, ranging from 8.0 to 10.7 Gt CO_2 in 2012. NJU has the highest emissions during the periods of 2005—2015, followed by EDGAR, MEIC and CDIAC/GCP/ODIAC, while CEADs (National) and PKU were much lower (Figure 2). This is mainly because of three reasons: 1) the EF for raw coal was higher for EDGAR and ODIAC than the others. The EFs were different for different fossil fuel types and cement production (Table S2). Since coal consumption consisted 70-80% of total emissions, coal EF is more significant than the others. The EFs were different for three major fossil fuel types (raw coal, oil and natural gas) and cement production (Table 1 and S2). And they are from either IPCC default values or local optimized values from different sources. They do not change over time in these inventories although they should, due to the unavailability of EFs over time; 2) differences in activity data, NJU, MEIC and CEADs (Provincial) used provincial data from CESY (2016), while CEADs (National), PKU used national data from CESY (2016) and IEA (2014), respectively (Table 1 and S1), and sum of provincial emissions would be higher than the national total; 3) differences in emission definitions (Table 1 and S1, emissions sectors). Although we tried to make these datasets as comparable as possible, there are still minor differences in emission sources (sectors). For example, EDGAR contains abundant industry processes emissions while CEADs only considered cement production (Janssens-Maenhout et al., 2019b). EDGAR and MEIC have a similar trend, but for magnitude, MEIC is usually higher than EDGAR. This is a combined effect of the above three reasons. MEIC used provincial energy data CESY (2016) while EDGAR used national level IEA (2014). But MEIC's EF is lower than EDGAR. These opposing effects would bring them closer in magnitude. The gridded products (ODIAC, EDGAR, MEIC and NJU) and national inventory (GCP/CDIAC) both show small differences in magnitude of total emissions estimates and trend from 2000—2007, and the differences in magnitude increased gradually from 2008 onward. Although the range increased with time, the relative difference remains at around 21% of the corresponding years' total

estimates, indicating potential systematical differences such as that EFs remain stable.

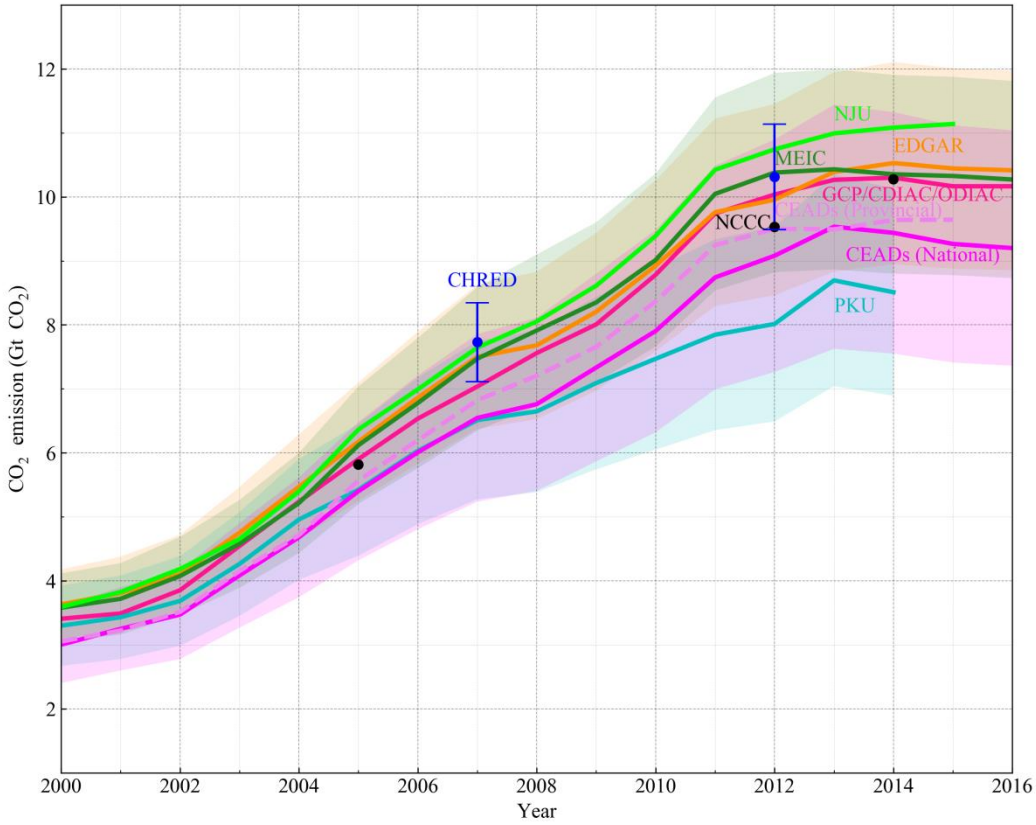

Figure 2. China's total $FFCO_2$ emissions from 2000 to 2016. The emissions are from combustion of fossil fuels and cement production from different sources (EDGARv4.3.2_FT2016 includes international aviation and marine bunkers emissions). To keep comparability and avoid differences resulted from the emissions disaggregation (e.g. Oda et al. 2018(Oda et al., 2018)). The values for 6 gridded emission inventories are tabular data provided by data developers before spatial disaggregation. Prior to 2014, GCP data was taken from CDIAC and 2015-2016 was calculated based on BP data and fraction of cement production emissions in 2014. Shading area (error bar for CHRED) indicates uncertainties from coauthors' previous studies (See Table 1).

4.2 Spatial distribution of $FFCO_2$ emissions

The evaluation of spatially-explicit $FFCO_2$ emissions is fundamentally limited by the lack of direct physical measurements on grid scales (e.g. (Oda et al., 2018)). We thus attempted to characterize the spatial patterns of China's carbon emissions by presenting emission estimates available. We compared 6 gridded products including ODIAC, EDGAR, PKU, CHRED, MEIC and NJU in 2012. The year 2012 was the most recent year for which all the six datasets were available. Spatially, CO_2 emissions from different datasets are concentrated in eastern China (Figure 3). High emission areas were mostly distributed in city clusters (e.g. BeijingTianjin-Hebei (Jing-Jin-Ji), the Yangtze River Delta, and the Pearl River Delta) and densely populated areas (e.g. the North China Plain, the Northeast China Plain and Sichuan Basin). These major spatial patterns are primarily due to the use of spatial proxy data, and also in accordance with previous studies (Guan et al., 2018;Shan et al., 2018). However, there were notable differences among different estimates at finer spatial scales. The large carbon emission regions were found in the North China Plain and the Northeast China Plain for ODIAC (Figure 3a), PKU (Figure 3c), MEIC

(Figure 3e) and NJU (Figure 3f), which ranged from 1000 to 10, 000 t CO_2/km^2. However, the high emissions located in the Sichuan Basin were found from PKU, MEIC and NJU, but not from ODIAC. This discrepancy in identifying the large CO_2 emissions was probably due to the emissions from rural settlements with high population densities (e.g. Sichuan Basin), did not appear strongly in satellite nighttime lights and ODIAC map (Wang et al., 2013). The more diffusive distribution for MEIC and NJU is attributed to the point sources abundance, with or without line sources and area sources proxies. Besides, EDGAR, PKU, CHRED, MEIC and NJU all showed relatively low emissions in western China, but the emission from ODIAC was zero due to no nighttime light there, which tended to distribute more emissions towards strong nightlights urban regions (Wang et al., 2013).

EDGAR, CHRED and MEIC all showed the traffic line source emissions by inducing traffic networks in spatial disaggregation. The line emissions (such as expressway, arterial highway) depicted a more detailed spatial distribution in CHRED than EDGAR and MEIC. This discrepancy could be attributed to the different road networks and corresponding weighting factors they used. CHRED disaggregated emissions from the transport sector based on traffic networks and traffic flows (Cai et al., 2018). MEIC applied the traffic network from the China Digital Road-network Map (CDRM) (Zheng et al., 2017), and EDGAR traffic networks were obtained from the OpenStreetMap and OpenRailwayMap (Geofabrik, 2015). ODIAC considered point and area sources and was lack of line source emissions in spatial disaggregation, which would put more emissions towards populated areas than suburbs (Oda et al., 2018). Oda and Maksyutov (2011) (Oda and Maksyutov, 2011) pointed out the possible utility of the street lights to represent line source spatial distributions even without the specific traffic spatial data. The spatial distributions of traffic emissions are highly uncertain with biases of 100% or more (Gately et al., 2015), which is due largely to mismatches between downscaling proxies and the actual vehicle activity distribution.

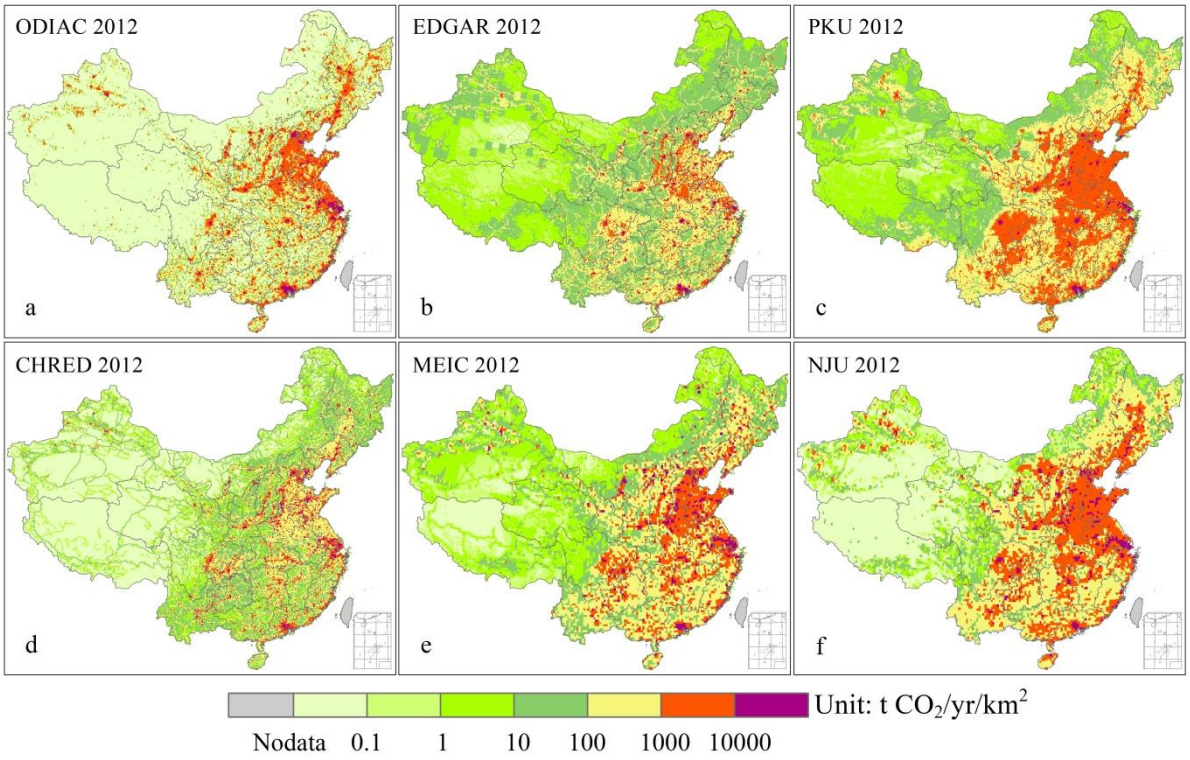

Figure 3. Spatial distributions of ODIAC (a), EDGAR (b), PKU (c), CHRED (d), MEIC (e) and NJU (f) at 10 km resolution for 2012. ODIAC was aggregated from 1 km data, MEIC, PKU, and EDGAR was resampled from 0.25, 0.1 and 0.1 degree.

4.3 CO_2 emissions at provincial level

The provincial level results showed more consistency than the grid level in spatial distribution. All products agree that eastern and southern provinces are high emitters (>400 Mt CO_2/yr, Figure 4 and S3), and western provinces were low emitters (<200 Mt CO_2/yr, Figure 4 and S3). The top 5 emitting provinces were Shandong, Jiangsu, Hebei, Henan, and Inner Mongolia with the amount ranging from 577 ± 48 Mt to 820 ± 102 Mt CO_2 in 2012 (Figure 4). While provinces located in western area with low economic activity and population density showed low carbon emissions (<200 Mt CO2, Figure 4 and S3). There is a clear discrepancy in provincial-level emissions among different estimates, and the mean standard deviation (SD) for 31 provinces' emissions was 62 Mt CO_2 (or 20%) in 2012. A large SD (>100 Mt CO2) occurs in high emitting provinces, such as Shandong, Jiangsu, Inner Mongolia, Shanxi, Hebei, and Liaoning. For Shandong province, the inventories vary from 675-965 Mt CO_2/yr, with a relative SD of 12% (Figure 4 and 5), and for other high emitting provinces the relative SD ranged 12% - 48%. This implied that there is still room to reduce uncertainty.

Since estimates based on provincial energy statistics are assumed to be more accurate than those derived from disaggregation

of national total using spatial proxies, we evaluated the provincial emissions of each inventory using the provincial-based inventory mean (CHRED, MEIC, and NJU) (Figure 5). The results showed that emissions derived from the provincial energy statistics are highly correlated, with R ranging from 0.99 to 1.00 and slope ranging 0.96 to 1.04. By contrast, the estimates for ODIAC, EDGAR, and PKU which used IEA national energy statistics, showed an obvious disparity, especially in the top 5 emitting provinces, suggesting the large impact of spatial disaggregated approaches in allocating total emissions. The potential implication is when doing spatial disaggregation, national-data-based inventories can use provincial fractions as constraints.

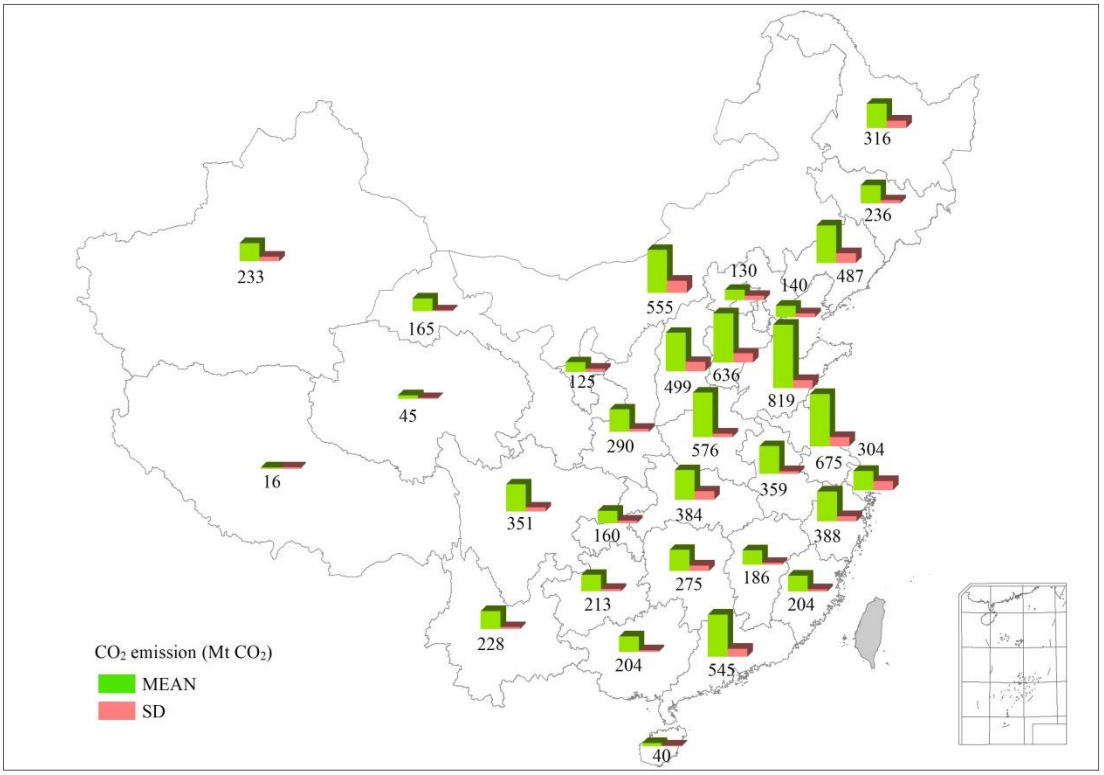

Figure 4. Provincial mean total emissions for ODIAC, EDGAR, PKU, CHRED, MEIC and NJU in 2012. Numbers refer to the green bar are provincial total CO_2 emissions in Mt.

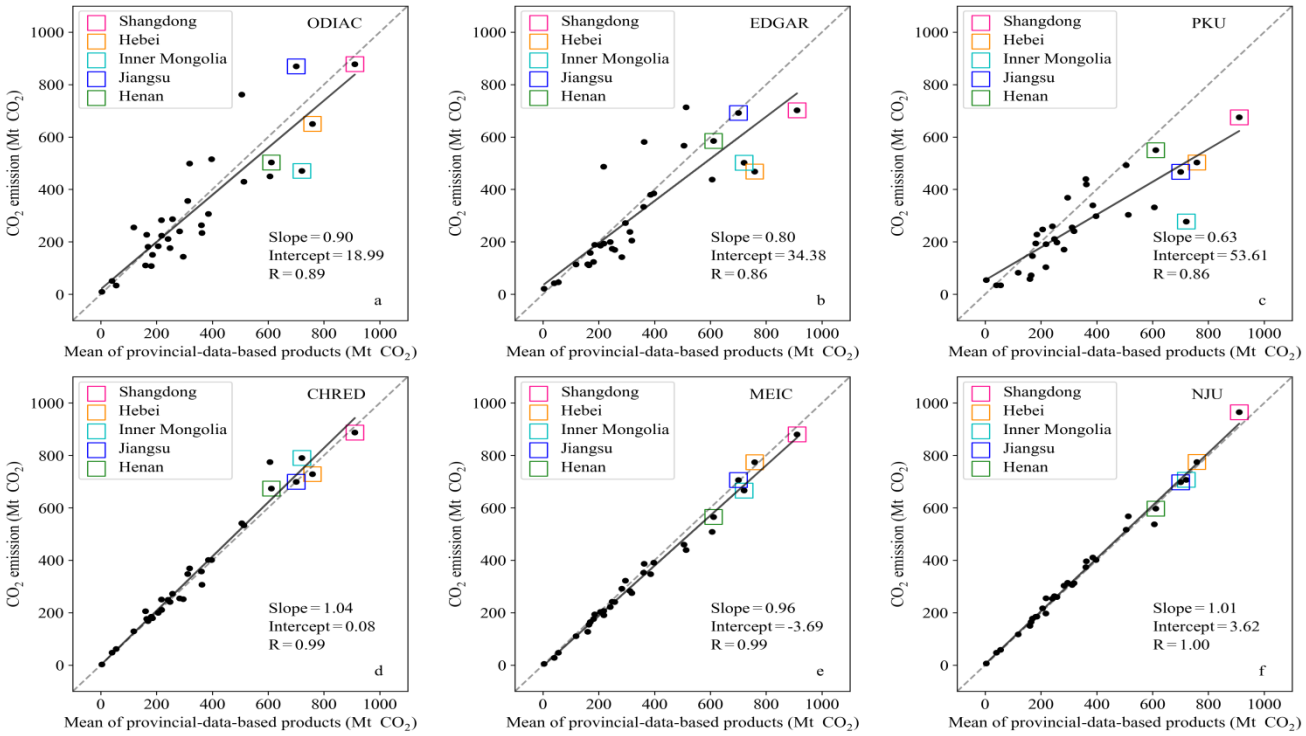

Figure 5. Scatter plots of provincial total emissions for ODIAC, EDGAR, PKU, CHRED, MEIC and NJU in 2012 with top 5 provinces highlighted, and the x axis is the mean of provincial-data-based products (CHRED, MEIC and NJU).

4.4 Statistics of CO_2 emissions at grid level

To further characterize the spatial pattern of China's CO_2 emissions, the probability density function (PDF), cumulative emissions, and top 5% emitting grids were analyzed to identify the spatial differences from the distribution of grid cell emissions (Figure 6). As illustrated in Figure 4a, ODIAC showed a large number of cells with zero emissions (62%) (Figure 6a), medium emitting grids (500-50000 t CO_2/km^2) consisted 30%, while high emitting grids (>50000 t CO_2/km^2) consisted 3%. While low emissions cells (1 ~ 500 t CO_2/km^2) were mainly located in EDGAR (58%) and CHRED (69%) (Figure 6b and d), and medium emitting grids consisted 30-40%, while high emitting grids consisted 2-3%. This could have a notable impact on cumulative national total emissions (Figure 6g). The frequency distribution of high emission grids revealed the different point source data. MEIC showed the largest number of high-emitting cells (500~500000 t CO_2/km^2, 5% compared with others 2-3%, Figure 6e) by using a high-resolution emission database (CPED) including more power plant information (Li et al., 2017;Liu et al., 2015a). Furthermore, ODIAC and EDGAR showed a good agreement in high emissions (> 100000 t CO_2/km^2), because their point source emissions were both from CARMA database (Table 1). Moreover, CARMA is the only global database for tracking CO_2 that gathered and presented the best available estimates of CO_2 emissions for 50,000 power plants around the world, of which around 15, 000 have latitude and longitude information with emissions larger than 0.

The database is responsible for about one-quarter of all greenhouse gas emissions. However, CARMA is no longer active (the last update was November 28, 2012), and the geolocations of power plants are not accurate enough, especially in China (Byers et al., 2019;Liu et al., 2013;Wang et al., 2013;Liu et al., 2015a). Therefore users have to do corrections themselves (Liu et al., 2013;Oda et al., 2018;Wang et al., 2013;Janssens-Maenhout et al., 2019b;Liu et al., 2015a).

As depicted by the cumulative emissions plot (Figure 6g), PKU and NJU showed very similar cumulative curves, and so did EDGAR and CHRED. Moreover, the total emissions for EDGAR and CHRED were largely determined by a small proportion of high emitting grids with a steep increase at the last stage of cumulative curves (Figure 6g), and the top 5% emitting grids accounted for ~90% of the total emissions (Figure 6e), higher than those of 82%, 71%, 58% and 51% in ODIAC, MEIC, NJU and PKU, respectively. The emissions from PKU, MEIC and NJU were relatively evenly distributed. This was due to CHRED was mainly derived from enterprise-level point sources (Cai et al., 2018). In contrast, the emissions of PKU showed the most even pattern, and the emissions from top 5% emitting grids only accounted for 51% (Figure 6g). This was because PKU had a special area source survey data for the Chinese rural areas from a 34,489-household energy-mix survey and a 1,670-household fuel-weighing campaign (Tao et al., 2018). Moreover, the spatial disaggregation proxy using population density also contributed to this spatial pattern. Similarly, MEIC and NJU exhibited a even distribution because of the same activity data from CESY, National Bureau of Statistics (Table 1).

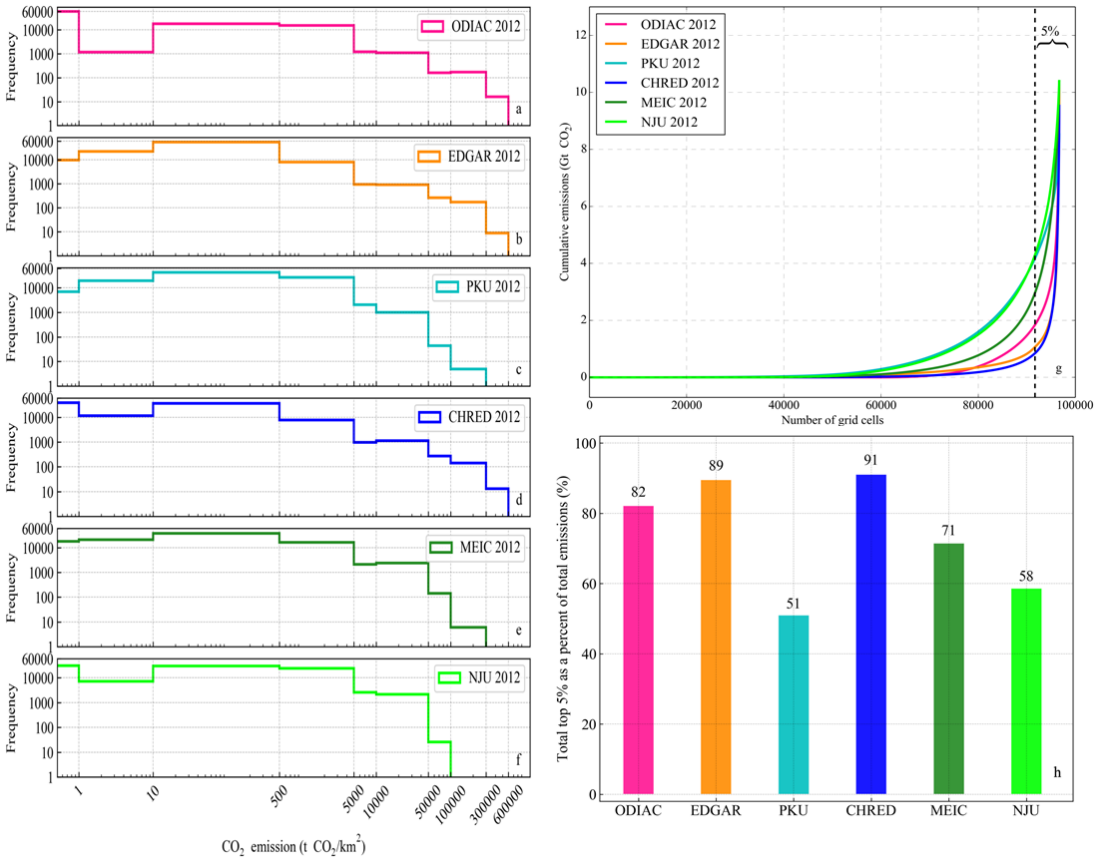

Figure 6. Frequency counts (a-f), cumulative emissions (g) (grids were sorted from low to high), and top 5% emitting grids plots (h) for ODIAC, EDGAR, PKU, CHRED, MEIC and NJU in 2012 at 10 km resolution.

To identify the locations of hotspots, the bubble plots (Figure S2) demonstrated the spatial distribution of high-emitting grid cells that were larger than 50 kt CO_2/km^2. CHRED, EDGAR and ODIAC showed a similar pattern, with high-emitting grids concentrated in city clusters (e.g. Jing-Jin-Ji, the Yangtze River Delta, and the Pearl River Delta) and the eastern coast (Figure S2). EDGAR and ODIAC both derived the power plant emissions from CARMA, but ODIAC was likely to put more emissions than EDGAR over urbanized regions with lights, especially in the North China Plain. The emissions of CPED and CARMA were similar in China with a minor difference of 2%, but the numbers of power plants had a large difference (2320 vs. 945) (Liu et al., 2015a). This implied that CARMA tended to allocate similar emissions to fewer plants than CPED.

5. Discussion

5.1 Activity data differences in datasets and their effects

Activity data source, data level and sectors determined the total emissions largely. As can be seen in Fig. 1, activity data and EF determine the total emission estimates, and then affect the spatial distributions through disaggregation proxies of point, line and area sources. It has been well-discussed that sum of provincial data is larger than the national total (Guan et al.,

2012;Hong et al., 2017;Liu et al., 2015b;Shan et al., 2018;Liu et al., 2013). CEADs (Provincial) is 8-18% higher than CEADs (National) after year 2008 (Figure 2). And thus province-based estimates (e.g. NJU and MEIC) are higher than CEADs (National). This could be attributed to the differences in national and provincial statistical systems and artificial factors, such as that some of provincial energy balance sheets were adjusted to make to achieve the exact match between supply and consumption (Hong et al., 2017). For example, the provincial statistics has data inconsistency and double counting problems (Qiang et al., 2007;Guan et al., 2012). One possible way to improve this is to use the provincial consumption fractions to rescale the national total consumptions when distributing emissions to grids. Hong et al. (2017) found that the ratio of the maximum discrepancy to the mean value was 16% due to different versions of national and provincial data in CESY. Ranges of 32-47% of CO_2 emissions from power sector (mainly coal use) were found among inventories, while for transport sector (mainly liquid fuels) the fractions ranged from 7-9%. Apart from such differences, one peak of FFCO2 emissions was identified by most dataset in 2013, which was due largely to the slowing economic growth (NBS, 1998–2017), changes in industrial structure (Mi et al., 2017;Guan et al., 2018) and a decline in the share of coal used for energy (Qi et al., 2016), and strategies for reducing emissions could be based on such uniformed trends, while making reduction policies for provinces needs the support of provincial-energy-based datasets instead of national-energy-based ones. Estimates with more sectors would usually be higher than those with fewer. For different emission sectors, EDGAR has international aviation and bunkers (Janssens-Maenhout et al., 2017) and NJU has wastes sector(Liu et al., 2013) (Table S1), and thus were higher than others. Moreover, for MEICv.1.3 downloaded from official website, it included biofuel combustion (which accounted for ~5.7% of the total), and the version used here was specially prepared to exclude biofuel to increase comparability. For another instance, CEADs industry processes only take account of cement production and was thus lower than those (e.g., NJU and EDGAR) with more processes (iron and steel, etc.) (Janssens-Maenhout et al., 2017;Shan et al., 2018;Liu et al., 2013). For PKU dataset, it used IEA energy statistics with more detailed energy sub-types. The emission factors was based on more detailed energy sub-types with lower EFs, and other inventories used average of large groups (Table 1) and sum of more detailed sub-types might not equal to the total of large groups due to incomplete of the statistics, and these could be reasons for its lower estimate (Wang et al., 2013). A further comparison with IEA, EIA and BP estimates with only energy related emissions also confirm that estimates with more sectors would be higher than those with fewer (Figure S1).

5.2 Emission factor effects on total emissions

Carbon emissions are calculated from activity data and EF, and the uncertainty in estimates is typically reported as 5% - 10%, while the maximum difference in this study reached 33.8% (or 2.7 PgC) in 2012. One major reason for this difference is the EF used by these inventories (Table 1). The EF for raw coal ranged from 0.491 to 0.746. For example, CEADs used 0.499 tC per ton of coal based on large-sample measurements, while EDGAR used 0.713 from the default values recommended by IPCC (Janssens-Maenhout et al., 2017;Liu et al., 2015b;Shan et al., 2018), and the differences are due largely to the low

quality and high ash content of Chinese coal. The variability of lignite and coal quality is quite large. In Liu et al., (2015) the carbon content of lignite ranged from 11% to 51% with mean±SD of 28%±13 (n=61). Furthermore, another study showed that the uncertainty from EF (-16 – 24%) was much higher than that from activity data (-1 – 9%) (Shan et al., 2018). We recommended substituting IPCC default coal EF with the CEADs EF. Regarding the plant-level emissions from coal consumptions, the collection of their EFs measured at fields representing the quality and type of various coals are highly needed to calibrate the large point source emissions, and we call for inclusion of physical measurements for calibration and validation of existing datasets (Bai et al., 2007;Dai et al., 2012;Kittner et al., 2018;Yao et al., 2019). Different fuel types would contribute differently to emission factors, i.e., for the same net heating value, natural gas emitted lowest carbon dioxide (61.7 kg CO2/TJ energy), followed by oil (65.3 kg CO2/TJ energy) and coal (94.6 kg CO2/TJ energy), and one successful example for reducing air pollutants and CO_2 was that the Chinese government initiated the "project of replacement of coal with natural gas and electricity in North China" in 2016 (Zheng et al., 2018a). Moreover, the non-oxidation fraction of 8% used in Liu et al. (2015) (Liu et al., 2015b) for coal was attributable to the differences comparing with a default non-oxidation fraction of 0% recommended by IPCC (2006) in EDGAR (Janssens-Maenhout et al., 2017). Moreover, averaged coal qualities are varying with time, yet we lacked such time-series quality data on raw coal. Bottom-up inventories typically use time-invariant EFs for CO_2 due to the lack of information on coal heating values over time and the MEIC model also uses constant EFs of CO_2 (Zheng et al., 2018). Teng and Zhu (2015) recommended time varied conversion factors from raw coal to standard coal, and change the raw coal to commodity coal in energy balance statistics since the latter has relatively efficient statistics on EF.

5.3 Spatial distribution of point, line and area sources

5.3.1 Point sources in datasets and the effects on spatial distribution

Point sources emissions account for a large proportion of total emissions (Hutchins et al., 2017). Power plants consumed about half of the total coal production in the past decade (Liu et al., 2015a). Thus, the accuracy of point sources was extremely important for improving emission estimates. ODIAC, EDGAR, and PKU all distributed power plant emissions from CARMA dataset. However, the geolocation errors in China are relatively large, and only 45% of power plants were located in the same $0.1 \times 0.1^\circ$ grid in CARMA v2.0 as the real power plants locations that were identified by eyeballing in google maps (Wang et al., 2013), because CARMA generally treats the city-center latitudes and longitudes as the approximate coordinates of the power plants (Wheeler and Ummel, 2008).

Liu et al. (2015a) found that CARMA neglected about 1300 small power plants in China. Thus CARMA allocated similar emissions to a limited number of plants than CPED (Table S2, 720, 1706 and 2320 point sources for ODIAC, EDGAR and MEIC, respectively), and ODIAC had fewer point sources due to elimination of wrong geolocations. The high-emitting grids in CHRED were attributed to the 1.58 million industrial enterprises from the First China Pollution Source Census (FCPSC)

used as point sources (Wang et al., 2014). Following the CARMA example, we call on the open source of large point sources for datasets and Chinese scientists need to adjust the locations of point sources from CARMA.

5.3.2 Effects of spatial disaggregation methods on line and area sources

Downscaling methods are widely used for its uniformity and simplicity because of the lack of detailed spatial data. Disaggregation methods used (e.g. nighttime light, population) by inventories strongly affect the spatial pattern. For example, ODIAC mainly use nighttime light from satellite to distribute emissions. Thus the hotspots concentrated more in strong nighttime light regions. However, using remote sensing data tended to underestimate industrial and transportation emissions (Ghosh et al., 2010). For instance, coal-fired power plants do not emit strong lights and may be far away from cities by transmission lines. Electricity generation and use are usually happened at different places, and stronger night-time light does not always mean higher CO_2 emissions (Cai et al., 2018;Doll et al., 2000). Furthermore, night time lights would ignore some other main fossil fuel emissions such as household cooking with coal. The good correlation between night-time light and CO_2 emissions is usually on a larger scale basis (national or continental) (Oda et al., 2010;Raupach et al., 2010), while this relationship would fail in populated or industrialized rural areas.

Transport networks are also used in several inventories for spatial disaggregation. EDGAR and CHRED both showed clear transport emissions especially in western China. EDGAR used three road types and corresponding weighting factors to disaggregate line source emissions. CHRED used national traffic networks and their flows to distribute traffic emissions (Cai et al., 2018;Cai et al., 2012). It is easier to obtain the traffic networks but rather difficult to get the traffic flows and vehicle kilometers travelled (VKT) data, and thus the weighting factors method are much easier to apply.

Population is widely used in spatial disaggregation (Andres et al., 2014;Andres et al., 2016;Janssens-Maenhout et al., 2017). The CDIAC emission maps originally used a static population data to distribute emissions and recently have changed to a temporally varying population proxy, which largely reduced the uncertainty. However, the unified algorithm for spatial disaggregation such as population density approach has difficulties in depicting the uneven development of rural and urban areas, and it usually use interpolation for limited base years and does not truly vary across years at high spatial resolution (Andres et al., 2014). Furthermore, downscaling approaches may introduce approximately 50% error per pixel, which are spatially correlated (Rayner et al., 2010), and this problem needs to be considered in future studies.

Moreover, big cities virtually eliminated use of coal (Guan et al., 2018;Zheng et al., 2018a), while in rural areas use of coal even increased (Meng et al., 2019). For example, a national survey showed that China's rural residential coal consumption fractions for heating increased from 19.2% to 27.2% (Tao et al., 2018). These transitions has impacts on spatial distribution of both CO_2 and air pollutants. And the high resolution CO_2 emissions have a potential proxy for fossil fuel emissions (Wang et al., 2013), thus further improvements on spatial disaggregation should consider these transitions and the surveyed data.

Data availability. The data sets of ODIAC, EDGAR, PKU and CEADs are freely available from http://db.cger.nies.go.jp/dataset/ODIAC/, http://edgar.jrc.ec.europa.eu/overview.php?v=432_GHG&SECURE=123, http://inventory.pku.edu.cn/download/download.html and http://www.ceads.net/ respectively. And CHRED, MEIC and NJU are available from data developers upon request.

Author contributions. PFH and NZ conceived and designed the study. PFH and XHL collected and analyzed the data sets. PFH, XHL, NZ and TO led the paper writing with contributions from all coauthors.

Competing interests. The authors declare that they have no conflict of interest.

Acknowledgments. This work was supported by National Key R&D Program of China (No. 2017YFB0504000). We thank Dr. Bofeng Cai from Chinese Academy for Environmental Planning for kindly providing CHRED data and his suggestions for improving the manuscript.

Supporting Information. Data and methodology descriptions on the 9 datasets and supplementary figures on emission estimates

References

Andres, R. J., Gregg, J. S., Losey, L., Marland, G., and Boden, T. A.: Monthly, global emissions of carbon dioxide from fossil fuel consumption, Tellus, 63, 309-327, 2011.

Andres, R. J., Boden, T. A., Bréon, F. M., and Ciais, P.: A synthesis of carbon dioxide emissions from fossil-fuel combustion, Biogeosciences,9,5(2012-05-25), 9, 1845-1871, 2012.

Andres, R. J., Boden, T. A., and Higdon, D.: A new evaluation of the uncertainty associated with CDIAC estimates of fossil fuel carbon dioxide emission, Tellus B: Chemical and Physical Meteorology, 66, 23616, 10.3402/tellusb.v66.23616, 2014.

Andres, R. J., Boden, T. A., and Higdon, D. M.: Gridded uncertainty in fossil fuel carbon dioxide emission maps, a CDIAC example, Atmospheric Chemistry & Physics, 16, 1-56, 2016.

Bai, X. F., Wen-Hua, L. I., Chen, Y. F., and Jiang, Y.: The general distributions of trace elements in Chinese coals, Coal Quality Technology, 2007.

Bao, Z., Han, P., Zeng, N., Liu, D., Wang, Y., Tang, G., Yao, B., and Zheng, K.: Observation and modeling of vertical carbon dioxide distribution in a heavily polluted suburban environment, Atmospheric and Oceanic Science Letters, 10.1080/16742834.2020.1746627, 2020.

Berezin, E. V., Konovalov, I. B., Ciais, P., Richter, A., Tao, S., Janssens-Maenhout, G., Beekmann, M., and Schulze, E.-D.: Multiannual changes of CO2 emissions in China: indirect estimates derived from satellite measurements of tropospheric NO2 columns, Atmos. Chem. Phys., 13, 9415-9438, https://doi.org/9410.5194/acp-9413-9415-2013, 2013.

Boden, T. A., Marland, G., and Andres, R. J.: Global, Regional, and National Fossil-Fuel CO2 Emissions, Carbon Diox-ide Information Analysis Center, Oak Ridge National Labo-ratory, U.S. Department of Energy, Oak Ridge, Tenn., USA, https://doi.org/10.3334/CDIAC/00001_V2016, in, 2016.

Byers, L., Friedrich, J., Hennig, R., Kressig, A., Li, X., McCormick, C., and Malaguzzi, V. L.: A Global Database of Power Plants, in, World Resources Institute. Available online at www.wri.org/publication/global-database-power-plants., Washington, DC, 2019.

Cai, B., Yang, W., Cao, D., Liu, L., Zhou, Y., and Zhang, Z.: Estimates of China's national and regional transport sector CO 2 emissions in 2007, Energy Policy, 41, 474-483, 2012.

Cai, B., Liang, S., Zhou, J., Wang, J., Cao, L., Qu, S., Xu, M., and Yang, Z.: China high resolution emission database (CHRED) with point emission sources, gridded emission data, and supplementary socioeconomic data, Resources, Conservation and Recycling, 129, 232-239, https://doi.org/10.1016/j.resconrec.2017.10.036, 2018.

Dai, S., Ren, D., Chou, C.-L., Finkelman, R. B., Seredin, V. V., and Zhou, Y.: Geochemistry of trace elements in Chinese coals: A review of abundances, genetic types, impacts on human health, and industrial utilization, International Journal of Coal Geology, 94, 3-21, https://doi.org/10.1016/j.coal.2011.02.003, 2012.

Doll, C. H., Muller, J.-P., and Elvidge, C. D.: Night-time Imagery as a Tool for Global Mapping of Socioeconomic Parameters and Greenhouse Gas Emissions, AMBIO: A Journal of the Human Environment, 29, 157-162, 10.1579/0044-7447-29.3.157, 2000.

Gately, C. K., Hutyra, L. R., and Sue Wing, I.: Cities, traffic, and CO₂: A multidecadal assessment of trends, drivers, and scaling relationships, Proceedings of the National Academy of Sciences, 112, 4999-5004, 10.1073/pnas.1421723112, 2015.

Geofabrik: Openstreetmap, https://www.openstreetmap.org and OpenRailwayMap, 2015.

Ghosh, T., Elvidge, C. D., Sutton, P. C., Baugh, K. E., Ziskin, D., and Tuttle, B. T.: Creating a Global Grid of Distributed Fossil Fuel CO2 Emissions from Nighttime Satellite Imagery, Energies, 3, 1895, 2010.

Guan, D., Liu, Z., Geng, Y., Lindner, S., and Hubacek, K.: The gigatonne gap in China's carbon dioxide inventories, Nature Climate Change, 2, 672-675, 10.1038/nclimate1560, 2012.

Guan, D., Meng, J., Reiner, D. M., Zhang, N., Shan, Y., Mi, Z., Shao, S., Liu, Z., Zhang, Q., and Davis, S. J.: Structural decline in China's CO2 emissions through transitions in industry and energy systems, Nature Geoscience, 11, 551-555, 10.1038/s41561-018-0161-1, 2018.

Han, P., Lin, X., Zeng, N., Oda, T., Zhang, W., Liu, D., Cai, Q. C., Crippa, M., Guan, D., Ma, X., Janssens-Maenhout, G., Meng, W., Shan, Y., Tao, S., Wang, G., Wang, H., Wang, R., Wu, L., Zhang, Q., Zhao, F., and Zheng, B.: Province-level fossil fuel CO2 emission estimates for China based on seven inventories (Accepted), Journal of Cleaner Production, 2020.

Hong, C., Zhang, Q., He, K., Guan, D., Li, M., Liu, F., and Zheng, B.: Variations of China's emission estimates: response to uncertainties in energy statistics, Atmos. Chem. Phys., 17, 1227-1239, https://doi.org/1210.5194/acp-1217-1227-2017, 2017.

Hutchins, M. G., Colby, J. D., Marland, G., and Marland, E.: A comparison of five high-resolution spatially-explicit, fossil-fuel, carbon dioxide emission inventories for the United States, Mitigation and Adaptation Strategies for Global Change, 22, 947. https://doi.org/910.1007/s11027-11016-19709-11029, 2017.

IEA: Energy Balances of OECD and non-OECD countries, International Energy Agency, Paris, Beyond 2020 Online Database, in, 2014.

IPCC: IPCC Guidelines for National Greenhouse Gas Inventories. Eggleston, S., Buendia, L., Miwa, K., Ngara, T., Tanabe, K. (eds.). , IPCC-TSU NGGIP, IGES, Hayama, Japan. www.ipcc-nggip.iges.or.jp/public/2006gl/index.html, 2007.

IPCC AR5: IPCC 2013: the physical science basis. Contribution of Working Group I to the Fifth Assessment Report of the Intergovernmental Panel on Climate Change, in, edited by: Stocker, T., Qin, D., Plattner, G., Tignorand, M., Allen, S., Boschungand, J., Nauels, A., Xia, Y., Bex, V., and Midgley, P., Cambridge University Press, Cambridge, UK, 2013.

Janssens-Maenhout, G., Crippa, M., Guizzardi, D., Muntean, M., Schaaf, E., Dentener, F., Bergamaschi, P., Pagliari, V., Olivier, J. G. J., Peters, J. A. H. W., van Aardenne, J. A., Monni, S., Doering, U., and Petrescu, A. M. R.: EDGAR v4.3.2 Global Atlas of the three major Greenhouse Gas Emissions for the period 1970–2012, Earth Syst. Sci. Data Discuss., https://doi.org/10.5194/essd-2017-5179, 2017.

Janssens-Maenhout, G., Crippa, M., Guizzardi, D., Muntean, M., Schaaf, E., Dentener, F., Bergamaschi, P., Pagliari, V., Olivier, J. G., and Peters, J. A.: EDGAR v4. 3.2 Global Atlas of the three major greenhouse gas emissions for the period 1970–2012, Earth System Science Data, 11, 959-1002, 2019a.

Janssens-Maenhout, G., Crippa, M., Guizzardi, D., Muntean, M., Schaaf, E., Dentener, F., Bergamaschi, P., Pagliari, V., Olivier, J. G. J., Peters, J. A. H. W., van Aardenne, J. A., Monni, S., Doering, U., Petrescu, A. M. R., Solazzo, E., and Oreggioni, G. D.: EDGAR v4.3.2 Global Atlas of the three major greenhouse gas emissions for the period 1970–2012, Earth Syst. Sci. Data, 11, 959-1002, 10.5194/essd-11-959-2019, 2019b.

Kittner, N., Fadadu, R. P., Buckley, H. L., Schwarzman, M. R., and Kammen, D. M.: Trace Metal Content of Coal Exacerbates Air-Pollution-Related Health Risks: The Case of Lignite Coal in Kosovo, Environmental Science & Technology, 52, 2359-2367, 10.1021/acs.est.7b04254, 2018.

Le Quéré, C., Andrew, R. M., Friedlingstein, P., Sitch, S., Pongratz, J., Manning, A. C., Korsbakken, J. I., Peters, G. P., Canadell, J. G., Jackson, R. B., Boden, T. A., Tans, P. P., Andrews, O. D., Arora, V. K., Bakker,

D. C. E., Barbero, L., Becker, M., Betts, R. A., Bopp, L., Chevallier, F., Chini, L. P., Ciais, P., Cosca, C. E., Cross, J., Currie, K., Gasser, T., Harris, I., Hauck, J., Haverd, V., Houghton, R. A., Hunt, C. W., Hurtt, G., Ilyina, T., Jain, A. K., Kato, E., Kautz, M., Keeling, R. F., Klein Goldewijk, K., Körtzinger, A., Landschützer, P., Lefèvre, N., Lenton, A., Lienert, S., Lima, I., Lombardozzi, D., Metzl, N., Millero, F., Monteiro, P. M. S., Munro, D. R., Nabel, J. E. M. S., Nakaoka, S.-I., Nojiri, Y., Padin, X. A., Peregon, A., Pfeil, B., Pierrot, D., Poulter, B., Rehder, G., Reimer, J., Rödenbeck, C., Schwinger, J., Séférian, R., Skjelvan, I., Stocker, B. D., Tian, H., Tilbrook, B., Tubiello, F. N., van der Laan-Luijkx, I. T., van der Werf, G. R., van Heuven, S., Viovy, N., Vuichard, N., Walker, A. P., Watson, A. J., Wiltshire, A. J., Zaehle, S., and Zhu, D.: Global Carbon Budget 2017, Earth Syst. Sci. Data, 10, 405-448, https://doi.org/410.5194/essd-5110-5405-2018, 2018.

Lei, Y., Zhang, Q., Nielsen, C., and He, K.: An inventory of primary air pollutants and CO2 emissions from cement production in China, 1990–2020, Atmospheric Environment, 45, 147-154, https://doi.org/10.1016/j.atmosenv.2010.09.034, 2011.

Li, M., Zhang, Q., Kurokawa, J.-I., Woo, J.-H., He, K., Lu, Z., Ohara, T., Song, Y., Streets, D. G., Carmichael, G. R., Cheng, Y., Hong, C., Huo, H., Jiang, X., Kang, S., Liu, F., Su, H., and Zheng, B.: MIX: a mosaic Asian anthropogenic emission inventory under the international collaboration framework of the MICS-Asia and HTAP, Atmos. Chem. Phys., 17, 2017.

Liu, F., Zhang, Q., Tong, D., Zheng, B., Li, M., Huo, H., and He, K. B.: High-resolution inventory of technologies, activities, and emissions of coal-fired power plants in China from 1990 to 2010, Atmos. Chem. Phys., 15, 13299-13317, 2015a.

Liu, M., Wang, H., Wang, H., Oda, T., Zhao, Y., Yang, X., Zang, R., Zang, B., Bi, J., and Chen, J.: Refined estimate of China's CO2 emissions in spatiotemporal distributions, Atmos. Chem. Phys., 13, 10873-10882, https://doi.org/10810.15194/acp-10813-10873-12013, 2013.

Liu, Z., Guan, D., Wei, W., Davis, S. J., Ciais, P., Bai, J., Peng, S., Zhang, Q., Hubacek, K., Marland, G., Andres, R. J., Crawford-Brown, D., Lin, J., Zhao, H., Hong, C., Boden, T. A., Feng, K., Peters, G. P., Xi, F., Liu, J., Li, Y., Zhao, Y., Zeng, N., and He, K.: Reduced carbon emission estimates from fossil fuel combustion and cement production in China, Nature, 524, 335, 10.1038/nature14677 https://www.nature.com/articles/nature14677#supplementary-information, 2015b.

Marland, G., Hamal, K., and Jonas, M.: How Uncertain Are Estimates of CO2 Emissions?, Journal of Industrial Ecology, 13, 4-7, 2010.

Meng, W., Zhong, Q., Chen, Y., Shen, H., Yun, X., Smith, K. R., Li, B., Liu, J., Wang, X., Ma, J., Cheng, H., Zeng, E. Y., Guan, D., Russell, A. G., and Tao, S.: Energy and air pollution benefits of household fuel policies in northern China, Proceedings of the National Academy of Sciences, 116, 16773, 10.1073/pnas.1904182116, 2019.

Mi, Z., Meng, J., Guan, D., Shan, Y., Liu, Z., Wang, Y., Feng, K., and Wei, Y.-M.: Pattern changes in determinants of Chinese emissions, Environmental Research Letters, 12, 074003, 10.1088/1748-9326/aa69cf, 2017.

NBS, N. B. o. S. o. t. P. s. R. o. C.: China Statistical Yearbook 1998–2016, China Statistics Press, 1998–2017.

NDRC: The People's Republic of China Second National Communication on Climate Change, http://qhs.ndrc.gov.cn/zcfg/201404/W020140415316896599816.pdf, 2012a.

NDRC: Guidelines for China's Provincial GHG Emission Inventories, in, 2012b.

Oda, T., Maksyutov, S., and Elvidge, C. D.: Disaggregation of national fossil fuel CO2 emissions using a global power plant database and DMSP nightlight data, Proc. of the 30th Asia-Pacific Advanced Network Meeting, 220–229, 2010.

Oda, T., and Maksyutov, S.: A very high-resolution (1 km×1 km) global fossil fuel CO2 emission inventory derived using a point source database and satellite observations of nighttime lights, Atmos. Chem. Phys., 11, 543-556, https://doi.org/510.5194/acp-5111-5543-2011, 2011.

Oda, T., Maksyutov, S., and Andres, R. J.: The Open-source Data Inventory for Anthropogenic CO2, version 2016 (ODIAC2016): a global monthly fossil fuel CO2 gridded emissions data product for tracer transport simulations and surface flux inversions, Earth Syst. Sci. Data, 10, 87-107, https://doi.org/110.5194/essd-5110-5187-2018, 2018.

Olivier, J. G. J., Janssens‐Maenhout, G., Muntean, M., and Peters, J. A. H. W.: Trends in global CO2 emissions: 2014 report, JRC93171/PBL1490 report, ISBN: 978-994-91506-91587-91501, 2014.

Qi, Y., Stern, N., Wu, T., Lu, J., and Green, F.: China's post-coal growth, Nature Geoscience, 9, 564-566, 10.1038/ngeo2777, 2016.

Qiang, Z., Streets, D. G., He, K., and Klimont, Z.: Major components of China's anthropogenic primary particulate emissions, Environmental Research Letters, 2, 045027, 2007.

Qin, D., Ding, Y., and Mu, M.: Climate and Environmental Change in China: 1951–2012, in: Springer Environmental Science & Engineering, edited by: Qin, D., Ding, Y., and Mu, M., Springer-Verlag Berlin Heidelberg 2016, 2016.

Raupach, M. R., Rayner, P. J., and Paget, M.: Regional variations in spatial structure of nightlights, population density and fossil-fuel CO2 emissions, Energy Policy, 38, 4756-4764, https://doi.org/10.1016/j.enpol.2009.08.021, 2010.

Rayner, P. J., Raupach, M. R., Paget, M., Peylin, P., and Koffi, E.: A new global gridded data set of CO2 emissions from fossil fuel combustion: Methodology and evaluation, Journal of Geophysical Research Atmospheres, 115, doi:10.1029/2009JD013439, 2010.

SCIO, T. S. C. I. O. o. C.: Enhanced Actions on Climate Change: China's Intended Nationally Determined Contributions, http://www.scio.gov.cn/xwfbh/xwbfbh/wqfbh/33978/35364/xgzc35370/Document/1514539/1514539.htm, 2015.

Shan, Y., Liu, J., Liu, Z., Xu, X., Shao, S., Wang, P., and Guan, D.: New provincial CO2 emission inventories in China based on apparent energy consumption data and updated emission factors, Applied Energy, 184, 2016.

Shan, Y., Guan, D., Zheng, H., Ou, J., Li, Y., Meng, J., Mi, Z., Liu, Z., and Zhang, Q.: China CO2 emission accounts 1997-2015, Scientific Data, 5, 170201, 2018.

Statistics, N. B. o.: China Energy Statistical Yearbook 2016, China Statistics Press, Beijing, 2016.

Tao, S., Ru, M. Y., Du, W., Zhu, X., Zhong, Q. R., Li, B. G., Shen, G. F., Pan, X. L., Meng, W. J., Chen, Y. L., Shen, H. Z., Lin, N., Su, S., Zhuo, S. J., Huang, T. B., Xu, Y., Yun, X., Liu, J. F., Wang, X. L., Liu, W. X., Cheng, H. F., and Zhu, D. Q.: Quantifying the rural residential energy transition in China from 1992 to 2012 through a representative national survey, Nature Energy, 3, 567-573, 10.1038/s41560-018-0158-4, 2018.

Teng, F., and Zhu, S.: Which estimation is more accurate? A technical comments on Nature Paper by Liu et al on overestimation of China's emission, Science & Technology Review, 33, 112-116, 2015.

Wang, J., Bofeng, C., Lixiao, Z., Dong, C., Lancui, L., Ying, Z., Zhansheng, Z., and Wenbo, X.: High resolution carbon dioxide emission gridded data for China derived from point sources, Environmental Science & Technology, 48, 7085-7093, 2014.

Wang, M., and Cai, B.: A two-level comparison of CO2 emission data in China: Evidence from three gridded data sources, Journal of Cleaner Production, 148, 194-201,

https://doi.org/10.1016/j.jclepro.2017.02.003, 2017.
Wang, R., Tao, S., Ciais, P., Shen, H. Z., Huang, Y., Chen, H., Shen, G. F., Wang, B., Li, W., Zhang, Y. Y., Lu, Y., Zhu, D., Chen, Y. C., Liu, X. P., Wang, W. T., Wang, X. L., Liu, W. X., Li, B. G., and Piao, S. L.: High-resolution mapping of combustion processes and implications for CO2 emissions, Atmos. Chem. Phys., 13, 5189-5203, https://doi.org/5110.5194/acp-5113-5189-2013, 2013.
Wheeler, D., and Ummel, K.: Calculating CARMA: Global Estimation of CO2 Emissions from the Power Sector, Working Papers, 2008.
Yao, B., Cai, B., Kou, F., Yang, Y., Chen, X., Wong, D. S., Liu, L., Fang, S., Liu, H., Wang, H., Zhang, L., Li, J., and Kuang, G.: Estimating direct CO2 and CO emission factors for industrial rare earth metal electrolysis, Resources, Conservation and Recycling, 145, 261-267, https://doi.org/10.1016/j.resconrec.2019.02.019, 2019.
Zeng, N., Ding, Y., Pan, J., Wang, H., and Gregg, J.: Climate Change--the Chinese Challenge, Science, 319, 730-731, 10.1126/science.1153368, 2008.
Zheng, B., Zhang, Q., Tong, D., Chen, C., Hong, C., Li, M., Geng, G., Lei, Y., Huo, H., and He, K.: Resolution dependence of uncertainties in gridded emission inventories: a case study in Hebei, China, Atmos. Chem. Phys., 17, https://doi.org/10.5194/acp-17-921-2017, 2017.
Zheng, B., Tong, D., Li, M., Liu, F., Hong, C., Geng, G., Li, H., Li, X., Peng, L., Qi, J., Yan, L., Zhang, Y., Zhao, H., Zheng, Y., He, K., and Zhang, Q.: Trends in China's anthropogenic emissions since 2010 as the consequence of clean air actions, Atmos. Chem. Phys., 18, 14095-14111, https://doi.org/14010.15194/acp-14018-14095-12018, , 2018a.
Zheng, B., Zhang, Q., Davis, S. J., Ciais, P., Hong, C., Li, M., Liu, F., Tong, D., Li, H., and He, K.: Infrastructure Shapes Differences in the Carbon Intensities of Chinese Cities, Environmental Science & Technology, 52, 6032-6041, 10.1021/acs.est.7b05654, 2018b.